A polaronic approach to high-temperature, unconventional superconductivity

博　士　論　文

A polaronic approach to high-temperature, unconventional superconductivity
ポーラロン仲介による高温、非典型的超伝導理論の研究

金沢大学大学院自然科学研究科
物質化学専攻

学籍番号　：　1724022008
氏名　：　LIM FANG HAN
主任指導教員名　：　井田朋智
提出年月　：　2021 年 1 月 7 日

A route to phonon-mediated, high-temperature, unconventional superconductivity

Fang Han Lim[1]

[1]*Division of Material Chemistry, Graduate School of Natural Science and Technology, Kanazawa University, Kakuma-machi, Kanazawa, Japan, 920-1192.*

Abstract

We investigate the appearance of superconductivity in a model with Peierls electron-phonon coupling, for very low carrier concentrations. Superconductivity with very high critical temperatures occurs at all carrier concentrations if the electron-phonon coupling is not too weak, with a gap of $s + s^*$ symmetry that closes on the Fermi surface for appropriate parameters. The possibility of finding the elusive p-type superconductivity is also revealed, although this is not stable within the approximations we use. This work opens a new avenue in the search for room-temperature superconductivity at ambient pressures, based on a phonon glue.

PACS numbers:

Contents

I. INTRODUCTION

Over a century after its discovery [1], superconductivity (SC) remains a central theme in condensed matter and materials research. The main reason for this sustained interest is the challenge of finding whether room-temperature SC at ambient pressure is possible, and if yes, the mechanism(s) that enable it and the materials that exhibit it. A positive resolution to this challenge would result in revolutionary changes in most technology-driven aspects of our lives.

To date, the only universally accepted mechanism for SC is the Bardeen, Cooper and Schrieffer (BCS) theory [2], according to which the conventional, s-wave, low-T_C SC found in most elemental metals and simple alloys is due to weak electron-phonon coupling that overscreens the electron-electron repulsion, turning it into an effective attraction at low-energies. In the presence of a large Fermi sea, this weak attraction suffices to bind electrons into Cooper pairs below a low T_C, opening a small uniform gap in the density of states at the Fermi energy E_F. Because of the large density of Cooper pairs and their low mass, these effective bosons are phase coherent for all $T < T_C$, and hence superconduct. An upper limit for BCS $T_C < 30K$ was proposed about 50 years ago [3], however it keeps being revisited because of possible loopholes in the arguments [4].

Ever since, theorists have suggested ways to boost T_C, for example by using excitons as the glue [5, 6] or by including additional dynamical effect [7, 8]. This field exploded after the experimental discovery of high-T_C superconductivity in the cuprate family [9] and then in the iron-based families [10], which are classified as unconventional (non-BCS, not s-wave) superconductors. These are joined by other potentially uncoventional (and not yet fully understood) superconductors such as Sr_2RuO_4 [11] and other heavy fermions materials [12], K-doped $BaBiO_3$ [13] and weakly doped $SrTiO_3$ [14]. Several of these are thought to have a non-phononic glue, although the matter is still debated [15].

These findings suggest that there may be non-phononic mechanisms leading to higher-T_C superconductivity at ambient pressure [16], but they certainly need to be deciphered first, before we can attempt to figure out whether they allow for room-temperature T_C.

Instead of speculating about new glues, in this Letter we show that phonon-mediated superconductivity allows for unconventional high-T_C superconductivity if: (i) the system is in the antiadiabatic limit $\Omega \gg E_F$, where Ω is the characteristic phonon frequency; (ii) the

effective electron-phonon coupling is not too weak, $\lambda > 0.5$; and (iii) the electron-phonon coupling modulates the kinetic energy instead of the potential energy of the electron, *i.e.* it is of $g(\boldsymbol{k}, \boldsymbol{q})$ type like the Peierls model [17–20] and not of the $g(\boldsymbol{q})$ type like the much more studied Holstein and Fröhlich models [21, 22]. These three conditions open up to investigations a region of the parameter space that was not studied in the previous work, which was overwhelmingly focussed on the so-called Migdal-Eliashberg limit: $E_F \gg \Omega$ and $\lambda \ll 1$, and on the simpler, $g(\boldsymbol{q})$ mechanisms. The region of the parameter space we investigate is where "polaronic effects" become important, and indeed we show that they are responsible for the interesting behavior we uncover.

II. THEORY

In this section, we intend to brief readers the fundamental knowledge of condensed matter theory and superconductivity and also to introduce notations that will be used for the rest of the manuscript.

A. Second Quantization & Hamiltonians

At the end of 1800, when a number of experimental observations, such as radiation emission and absorption of black body could not be explained with existing physical laws, physicists are forced to look beyond the completely deterministic classical mechanics and elaborate new ideas that eventually produced a consistent body generally referred to as modern physics. In the meantime, modern physics that stemmed on the study of the microscopic world, has led to the development of quantum mechanics. Quantum mechanics is a fundamental theory to describe the physical properties of nature at the atomic or subatomic particles scale. As contrast with classical mechanics, the non-deterministic, probabilistic quantum mechanics shows that quantities like energy, and momentum etc. of a bounded system are restricted to discrete value (quantization). Starting with the duality of particles, the first quantization is a semi-classical treatment of quantum mechanics, in which particles or physical objects are treated using quantum wave functions that follows the Schrodinger equation,

$$\hat{H}\Psi = E\Psi \tag{1}$$

for the corresponding Hamiltonian H by replacing the canonical variables$(\hat{x}, \hat{p})$ that are conjugate to each other in analytical mechanics to

$$[\hat{x}, \hat{p}]_- = \hat{x}\hat{p} - \hat{p}\hat{x} = i\hbar \ , \tag{2}$$

but the surrounding environment (for example a potential well or a bulk electromagnetic field) is treated classically.

In this section, we discuss why working on a wavefunction which contains every information of a particle (First Quantization) is not ideal in solving many-body systems, especially when the number of particles in the system is not fixed.

1. Many-body state function in First Quantization

We can formulate the quantum mechanics for a single particle in some given representation, in terms of wave functions. If we generalize this approach to many-body systems of N particles, with the use of $x = (\boldsymbol{r}, \sigma)$, the many-body state function in the $\boldsymbol{r}$-representation is:

$$\langle x_1, x_2, \cdots, x_N | \Psi(t) \rangle = \Psi(x_1, x_2, \cdots, x_N, t) \, , \tag{3}$$

which is the amplitude of probability that at time t, particle 1 is at $x_1 = (\boldsymbol{r}_1, \sigma_1)$, etc.

First, for single particle, we always decompose wavefunctions in a given basis

$$\Psi(x,t) = \sum_\alpha c_\alpha(t) \langle x|\alpha\rangle = \sum_\alpha c_\alpha(t) \phi_\alpha(x). \tag{4}$$

This reduce the problem to that of working on the time-dependent complex number $c_\alpha(t)$. Here we use index α to denote the states of a complete single-particle basis (including the spin). Which basis to use depends on the problem at hand: for instance, for translationally invariant problems, we will use$\alpha = (\boldsymbol{k}, \sigma)$ as quantum numbers, whereas if we deal with an atom, we can use $\alpha = (n, l, m, \sigma)$ for its one-particle eigenstates.

If we have a complete basis for a single-particle Hilbert space, we can immediately generate a complete basis for the N-particle Hilbert space (the particles are identical), as the products of one-particle basis states, which is also called the Hartree product:

$$\Psi(x_1, x_2, \cdots, x_N, t) = \sum_{\alpha_1 \cdots \alpha_N} c_{\alpha_1 \cdots \alpha_N}(t) \phi_{\alpha_1}(x_1) \phi_{\alpha_2}(x_2) \cdots \phi_{\alpha_N}(x_N). \tag{5}$$

The Hartree Product is an uncorrelated wave function. Naturally, because the Hartree Product takes no account of the indistinguishability of electrons, it does not satisfy the principle of wave functions must be symmetric (for bosons) or antisymmetric (for fermions) to interchange of any identical particles.Because of this requirement, the physically meaningful many-body fermionic (bosonic) wave functions are from the antisymmetric (symmetric) sector of the N-particle Hilbert space, which we denote as:

$$\phi_{\alpha_1,\cdots,\alpha_N}(x_1,\cdots,x_N)=\sqrt{\frac{1}{N!\prod_i n_i!}}\sum_P \xi^P \phi_{\alpha_1}(x_{P_1})\,\phi_{\alpha_2}(x_{P_2})\cdots\phi_{\alpha_N}(x_{P_N}) \tag{6}$$

The factor in front is the normalization constant; n_i is the total number of particles in the same state α_i (only important for bosonic systems; in fermionic systems all $n_i = 1$ because of the Pauli's principle of exclusion), ξ is -1 (1) for fermionic (bosonic) system, P is its sign (number of transpositions),and the summation is over all possible permutations. For fermionic system, Eq.(6) is also referred as Slater determinant. Then the N-body wave function can be written as a linear combination of the properly antisymetrized/symmetrized basis states:

$$\Psi(x_1,x_2,\cdots,x_N,t)=\sum_{\alpha_1\cdots\alpha_N} c_{\alpha_1\cdots\alpha_N}(t)\,\phi_{\alpha_1,\cdots,\alpha_N}(x_1,\cdots,x_N) \tag{7}$$

Eq.(7) simply states that, even with only one single combination of one-particle states $\alpha_1,\cdots,\alpha_N$ is occupied, that is a single $\phi_{\alpha_1,\cdots,\alpha_N}(x_1,\cdots,x_N)$ basis wave function, this alone contains on the order of N! terms when we sum over all permutations in Eq.(6). This might not seems to be a problem for small N, However if $N \approx 10^{23}$ like we need to deal with for condensed matter systems, it becomes exceedingly troublesome, let alone working in grand-canonical ensemble where N is not fixed.

The origin of these complications is the fact that we insisted on working which wavefunctions which contain a lot of useless information (which particle is where). In fact, because the particles are indistinguishable, all we need to know is which one-particle states are occupied, and we do not need to bother listing which particle is where we know that all possible permutations will appear, anyway. Keeping only this minimal amount of necessary information is precisely what 2nd quantization does.

2. Second Quantization

Now we know that solving the Schrödinger Equation using many-body wave function in configuration space is impractical, we shall rely on second quantization. Starting with an abstract vector:

$$|n_1, n_2, ...\rangle \tag{8}$$

as being the state with n_1 particles in state "1" with index α_1, n_2 particles in state "2" with index α_2, etc. We have to list occupation numbers for all possible states for an empty state, $n_i = 0$. Of course, for fermionic systems we can only have n_i =0 or 1, for any i (Pauli's principle). For bosons, $n_i = 0, 1, 2, \cdots$ can be any non-negative integer. The ground-state for N non-interacting fermions is represented as $|1, 1, \cdots, 1, 0, 0, \cdots\rangle$ whereas the ground-state of a non-interacting bosonic system is $|N, 0, 0, \cdots\rangle$. The vacuum is$|0\rangle = |0, 0, \cdots\rangle$ in both cases.The ensemble of all possible states $\{|n_1, n_2, ...\rangle\}$ is a complete orthonormal basis of the so called Fock space.

To generate these abstract states, and also to work with operators so that computing their matrix elements is easy. We associate a pair of creation $c_\alpha^\dagger$ and annihilation c_α operator to each identical single-particle at state α which obey:

$$\begin{aligned}
&[c_\alpha, c_\beta^\dagger]_\xi = c_\alpha c_\beta^\dagger - \xi c_\beta^\dagger c_\alpha = \delta_{\alpha\beta} \\
&[c_\alpha^\dagger, c_\beta^\dagger]_\xi = [c_\alpha, c_\beta]_\xi = 0 \\
&\hat{n}_\alpha = c_\alpha^\dagger, c_\alpha,
\end{aligned} \tag{9}$$

where $\hat{n}_\alpha$ is the number operator, which tells us the number of particles in state α. From now on, we will call fermionic operators $a_\alpha^\dagger a_\alpha$ and bosonic operators $b_\alpha^\dagger b_\alpha$, we will only use $c_\alpha^\dagger c_\alpha$ when dealing with both types simultaneously.

For fermion, we get $a_\alpha^\dagger a_\alpha^\dagger = a_\alpha a_\alpha = 0$, because we can't create or annihilate two fermions wtih same state, i.e. the Pauli's principle of exclusion. So we found that

$$\begin{aligned}
a_{\alpha_1}^\dagger |0\rangle = |1\rangle \qquad , \qquad a|0\rangle = 0 \\
a_{\alpha_1}^\dagger |1\rangle = 0 \qquad , \qquad a_{\alpha_1}|1\rangle = |0\rangle .
\end{aligned} \tag{10}$$

For boson, bosonic operators obey $[b, b^\dagger] = 1$. Since the vacuum state contains no particles, we require that $b|0\rangle = 0$ for all single particle states. With n can be all non-negative

integers, we found that

$$b^\dagger |n\rangle = \sqrt{n+1}\,|n+1\rangle$$
$$b\,|n\rangle = \sqrt{n}\,|n-1\rangle\,.$$

With these creation ($c^\dagger$) and annihilation (c) operator, we can then define a general Fock basis state as an action of creation operator to the vacuum :

$$|n_1, n_2, ...\rangle = \frac{(c_1^\dagger)^{n_1}}{\sqrt{n_1!}}\frac{(c_2^\dagger)^{n_2}}{\sqrt{n_2!}}\cdots|0\rangle\,, \tag{11}$$

and the action of an annihilation operators on a Fock state can be written as below:

$$\begin{aligned} c_\alpha\,|n_1, \cdots, n_\alpha, \cdots\rangle &= c_\alpha \frac{(c_1^\dagger)^{n_1}}{\sqrt{n_1!}}\cdots\frac{(c_\alpha^\dagger)^{n_\alpha}}{\sqrt{n_\alpha!}}\cdots|0\rangle \\ &= \xi^P \frac{(c_1^\dagger)^{n_1}}{\sqrt{n_1!}}\cdots c_\alpha\frac{(c_\alpha^\dagger)^{n_\alpha}}{\sqrt{n_\alpha!}}\cdots|0\rangle \\ &= \xi^P\sqrt{n_\alpha}\,|n_1, \cdots, n_\alpha - 1, ...\rangle \end{aligned} \tag{12}$$

where P is the number of times c_α permute to the front of $c_\alpha^\dagger$. Similarly,

$$c_\alpha^\dagger\,|n_1, \cdots, n_\alpha, \cdots\rangle = \xi^P\sqrt{n_\alpha+1}\,|n_1, \cdots, n_\alpha + 1, ...\rangle\,. \tag{13}$$

Now we can start to reformulate the Schrödinger equation in the language of second quantization. In almost all of the cases, the Hamiltonian takes the form of

$$\begin{aligned} \hat{H} &= \hat{T} + \hat{V} \\ &= \sum_{i=1}^{N}\frac{\boldsymbol{p}_i}{2m} + \frac{1}{2}\sum_{i\neq j}u(\boldsymbol{r}_i - \boldsymbol{r}_j) \end{aligned} \tag{14}$$

in first quantization. Starting with the kinetic energy term, so that

$$\begin{aligned} \hat{T} &= \sum_{\alpha,\alpha'}\langle\alpha|\frac{p^2}{2m}|\alpha'\rangle\,c_\alpha^\dagger c_{\alpha'} \\ &= \sum_{\alpha,\alpha'}\sum_{\sigma}\int d\boldsymbol{r}\phi_\alpha^*(\boldsymbol{r},\sigma)\left(\frac{-\hbar^2}{2m}\nabla^2\right)\phi_\alpha(\boldsymbol{r}',\sigma')\,c_\alpha^\dagger c_{\alpha'} \end{aligned} \tag{15}$$

and asumming that the basis $\alpha = (\boldsymbol{k}, \sigma)$ are the eigenstates of the momentum operator, so that

$$\phi_{\boldsymbol{k},\sigma} = \delta_{\sigma,\sigma'}\frac{\exp(i\boldsymbol{k}\cdot\boldsymbol{r})}{\sqrt{V}} \tag{16}$$

is just plane-wave., where V is the volume of the system. Then Eq.(15) can be written as:

$$\begin{aligned}\hat{T} &= \sum_{\boldsymbol{k},\boldsymbol{k}',\sigma,\sigma'} \langle \boldsymbol{k},\sigma|\frac{p^2}{2m}|\boldsymbol{k}',\sigma'\rangle\, c^\dagger_{\boldsymbol{k},\sigma} c_{\boldsymbol{k},\sigma'} \\ &= \sum_{\boldsymbol{k},\boldsymbol{k}',\sigma,\sigma'} \delta_{\sigma,\sigma'}\delta_{\boldsymbol{k},\boldsymbol{k}'}\frac{\hbar^2 k^2}{2m} c^\dagger_{\boldsymbol{k},\sigma} c_{\boldsymbol{k}',\sigma'} \\ &= \sum_{\boldsymbol{k},\sigma} \frac{\hbar^2 k^2}{2m} c^\dagger_{\boldsymbol{k},\sigma} c_{\boldsymbol{k},\sigma} \end{aligned} \tag{17}$$

Next, before moving on to the two-particle operator , we first define the Fourier transform of the interaction potential

$$u(\boldsymbol{r}) = \frac{1}{V}\sum_{\boldsymbol{q}} \exp(i\boldsymbol{q}\cdot\boldsymbol{r}) u_{\boldsymbol{q}} \qquad , \qquad u_{\boldsymbol{q}} = \int d\boldsymbol{r} \exp(-i\boldsymbol{q}\cdot\boldsymbol{r}) u(r)\,, \tag{18}$$

with Eq.(18) and the orthonormality of spin function, we can write the interaction term as:

$$\begin{aligned}\hat{V} &= \frac{1}{2}\langle \boldsymbol{k}_1,\sigma_1;\boldsymbol{k}_2,\sigma_2|u|\boldsymbol{k}_3,\sigma_3;\boldsymbol{k}_4,\sigma_4\rangle\, c^\dagger_{\boldsymbol{k}_1,\sigma_1} c^\dagger_{\boldsymbol{k}_2,\sigma_2 a} c_{\boldsymbol{k}_4,\sigma_4} c_{\boldsymbol{k}_3,\sigma_3} \\ &= \frac{\delta_{\sigma_1,\sigma_3}\delta_{\sigma_2,\sigma_4}}{2}\int d\boldsymbol{r}_1 \int d\boldsymbol{r}_2 \frac{\exp\left(-i(\boldsymbol{k}_1\boldsymbol{r}_1 + \boldsymbol{k}_2\boldsymbol{r}_2)\right)}{V} u(\boldsymbol{r}_1-\boldsymbol{r}_2)\frac{\exp\left(i(\boldsymbol{k}_3\boldsymbol{r}_1 - \boldsymbol{k}_4\boldsymbol{r}_2)\right)}{V} \\ &\qquad \times c^\dagger_{\boldsymbol{k}_1,\sigma_1} c^\dagger_{\boldsymbol{k}_2,\sigma_2} c_{\boldsymbol{k}_4,\sigma_4} c_{\boldsymbol{k}_3,\sigma_3}\,,\end{aligned}$$

here we impose conditions $\boldsymbol{k}_1 = \boldsymbol{k}_3 + \boldsymbol{q}$, $\boldsymbol{k}_2 = \boldsymbol{k}_4 - \boldsymbol{q}$ for the exponential to vanish, and by changing the dummy variables $\boldsymbol{k}_3 = \boldsymbol{k}$, $\boldsymbol{k}_4 = \boldsymbol{k}'$, we found $\hat{V}$ as :

$$\hat{V} = \frac{1}{2V}\sum_{\substack{\boldsymbol{k},\boldsymbol{k}'\\ \sigma,\sigma'}}\sum_{\boldsymbol{q}} u_{\boldsymbol{q}} c^\dagger_{\boldsymbol{k}+\boldsymbol{q},\sigma} c^\dagger_{\boldsymbol{k}'-\boldsymbol{q},\sigma'} c_{\boldsymbol{k}',\sigma'} c_{\boldsymbol{k},\sigma} \tag{19}$$

Eq.(19) is saying that, the interaction between two particles that were in states $(\boldsymbol{k}',\sigma')$, $(\boldsymbol{k},\sigma)$ can be seen as a scattering process some momentum $\boldsymbol{q}$ transfer mediated by $u_{\boldsymbol{q}}$.

Thus, the Hamiltonian can finally be written down in second quantization formulation :

$$\hat{H} = \sum_{\boldsymbol{k},\sigma}\frac{\hbar^2 k^2}{2m} c^\dagger_{\boldsymbol{k},\sigma} c_{\boldsymbol{k},\sigma} + \frac{1}{2V}\sum_{\substack{\boldsymbol{k},\boldsymbol{k}'\\ \sigma,\sigma'}}\sum_{\boldsymbol{q}} u_{\boldsymbol{q}} c^\dagger_{\boldsymbol{k}+\boldsymbol{q},\sigma} c^\dagger_{\boldsymbol{k}'-\boldsymbol{q},\sigma'} c_{\boldsymbol{k}',\sigma'} c_{\boldsymbol{k},\sigma} \tag{20}$$

Likewise, we can also write the second-quantization expression for any operator, in terms of creation and annihilation operators.

3. The Jellium Model

The Jellium model is an approximation to quantum mechanical model of interacting electrons in a solid where the positive charges, i.e. atomic nuclei are assumed to be uniformly distributed in space; the electron density is a uniform quantity as well in space., resulting a translational invariant system. Within this system, only the behavior of the valence electrons needs to be understood.

In the first quantization, the Hamiltonian for this system is

$$\hat{H} = \hat{H}_{el} + \hat{H}_{bg} + \hat{H}_{el-bg}, \tag{21}$$

where the electronic Hamiltonian is

$$\hat{H}_{el} = \sum_{i=1}^{N} \frac{\boldsymbol{p}_i^2}{2m} + \frac{1}{2}\sum_{i\neq j} u(\boldsymbol{r}_i - \boldsymbol{r}_j) \tag{22}$$

where we will assume a so-called screened Coulomb interaction between electrons

$$u(\boldsymbol{r}) = \frac{e^2}{\boldsymbol{r}} \exp(-\mu \boldsymbol{r}) \tag{23}$$

The background has a uniform positive density n(r) = N=V , and its energy is:

$$\hat{H}_{bg} = \int d\boldsymbol{r} \int d\boldsymbol{r}' n(\boldsymbol{r}) u(\boldsymbol{r} - \boldsymbol{r}') n(\boldsymbol{r}') = \frac{N^2}{2V} u_{\boldsymbol{q}=0} \tag{24}$$

The electron-background interactions are described by:

$$\hat{H}_{el-bg} = -\sum_{i=1}^{N} \int d\boldsymbol{r} n(\boldsymbol{r}) u(\boldsymbol{r} - \boldsymbol{r}_i) = -\frac{N^2}{V} u_0 \tag{25}$$

because $\sum_i^1 = N$. So things simplify considerably because of the "jellium" assumption and we find:

$$\hat{H} = \sum_{i=1}^{N} \frac{\boldsymbol{p}_i^2}{2m} + \frac{1}{2}\sum_{i\neq j} u(\boldsymbol{r}_i - \boldsymbol{r}_j) - \frac{N^2}{2V} u_{\boldsymbol{q}=0}$$

We now go to the second quantization of Hamiltonian is:

$$\hat{H} = \sum_{\boldsymbol{k},\sigma} \frac{\hbar^2 k^2}{2m} c^\dagger_{\boldsymbol{k},\sigma} c_{\boldsymbol{k},\sigma} + \frac{1}{2V} \sum_{\substack{\boldsymbol{k},\boldsymbol{k}' \\ \sigma,\sigma'}} \sum_{\boldsymbol{q}} u_{\boldsymbol{q}} c^\dagger_{\boldsymbol{k}+\boldsymbol{q},\sigma} c^\dagger_{\boldsymbol{k}'-\boldsymbol{q},\sigma'} c_{\boldsymbol{k}',\sigma'} c_{\boldsymbol{k},\sigma} - \frac{N^2}{2V} u_{\boldsymbol{q}=0}$$

Let us consider the q = 0 contribution from the electron-electron interaction:

$$\frac{u_0}{2V} \sum_{\substack{\boldsymbol{k},\boldsymbol{k}' \\ \sigma,\sigma'}} \sum_{\boldsymbol{q}} c^\dagger_{\boldsymbol{k}+\boldsymbol{q},\sigma} c^\dagger_{\boldsymbol{k}'-\boldsymbol{q},\sigma'} c_{\boldsymbol{k}',\sigma'} c_{\boldsymbol{k},\sigma} - \frac{N^2}{2V} = \frac{u_0}{2V} \sum_{\substack{\boldsymbol{k},\boldsymbol{k}' \\ \sigma,\sigma'}} \sum_{\boldsymbol{q}} c^\dagger_{\boldsymbol{k}+\boldsymbol{q},\sigma} c_{\boldsymbol{k},\sigma} c^\dagger_{\boldsymbol{k}'-\boldsymbol{q},\sigma'} c_{\boldsymbol{k}',\sigma'} = \frac{N^2}{2V} u_0, \tag{26}$$

the $\boldsymbol{q} = 0$ contribution of $\hat{H}_{el}$ exactly cancels out contribution of $\hat{H}_{bg} + \hat{H}_{el-bg}$. So the total Hamiltonian for the Jellium model is

$$\hat{H} = \sum_{\boldsymbol{k},\sigma} \frac{\hbar^2 k^2}{2m} c^\dagger_{\boldsymbol{k},\sigma} c_{\boldsymbol{k},\sigma} + \frac{1}{2V} \sum_{\substack{\boldsymbol{k},\boldsymbol{k}' \\ \sigma,\sigma'}} \sum_{\boldsymbol{q}\neq 0} u_{\boldsymbol{q}} c^\dagger_{\boldsymbol{k}+\boldsymbol{q},\sigma} c^\dagger_{\boldsymbol{k}'-\boldsymbol{q},\sigma'} c_{\boldsymbol{k}',\sigma'} c_{\boldsymbol{k},\sigma} \tag{27}$$

4. The Hubbard Model

The Hubbard model has a long history, Gutzwiller and Hubbard have been actively researching the Hubbard model since 1963. At First, it was proposed as a model that take both the itinerant d-electrons that are responsible for magnetism and strong electron correlation into account. It was later used as a fundamental model to study the Mott-Hubbard type of metal-insulator transition. Furthermore, the Hubbard model is the simplest model in the theoretical research of strongly correlated electron systems, various discussions and developments are made based on the Hubbard model.

The Hubbard model considers only one electron orbital at each site, and its most common Hamiltonian is given by the following equation:

$$\hat{H} = -t \sum_{\langle i,j\rangle,\sigma} c^\dagger_{i,\sigma} c_{j,\sigma} + \sum_i U \hat{n}_{i,\uparrow} \hat{n}_{i,\downarrow}, \tag{28}$$

The first term is the kinetic energy term, the notation $\langle i, j\rangle$ shows that sum is over pairs of nearest-neighbor sites. The hopping integral t:

$$t_{ij} = \langle i,\sigma | Z \sum_{l\neq j} v\left(\boldsymbol{r} - \boldsymbol{R}_l\right) | j,\sigma\rangle \tag{29}$$

involves the hopping of an electron from one orbital of one atom into another orbital of the next atom, due to the attraction from the nuclei $l \neq j$ in the system. On the other hand, the second term is the on-site coulomb repulsion, since the strongest repulsion must be between electrons that belongs to the same nucleus. The Hubbard model mainly consider valence electrons, because these orbitals are usually only partially filled, so there are empty orbitals with the same energy into which electrons can be scattered by repulsion even if we keep on-site repulsion. Eq(28) is good enough to set up a model Hamiltonian, at temperature of 0K, we can adapt the Hubbard model to evaluate various physical properties by the changing three elements: 1.) The dimension and the crystal structure of the system 2.) The U/t ratio 3.) The electron concentration.

B. The Electronic Hamiltonian

In this section we discuss how to deal with electronic Hamiltonians. First we treat the ions as being frozen in their equilibrium positions, i.e. the Born-Oppenheimer approximation, so the electrons are moving in the resulting periodic potential and also experience electron-electron interaction. We will first ignore the electron-electron interactions, i.e. set them to zero. This allows us to study exactly model of non-interacting electrons moving in periodic potentials, to understand the typical aspects of electronic band-structures.

1. Non-interacting electrons in a periodic potential

For simplicity, let's assume that we put together many Li atoms ($1s^2 2s^1$ electronic structure) in a one dimensional chain, and we expect the $2s^1$ electrons to be the valence electrons, so we're considering 1 valence electron per Li^+ ion.We can label these with an index $n = 1, \cdots, N$, where we will let $N \to \infty$, in the end. Let a be the lattice constant, so the position of the nth ion is $R_n = n_a$. To describe the valence electrons, we introduce creation and annihilation operators $c^\dagger_{n,\sigma}, \quad c_{n,\sigma}$ for an electron at site n with spin σ.

This 2s orbital has some characteristic Bohr radius (a_B) over which it is spread away from its ion. Our approximation to keep only these orbitals is a reasonable approximation if the distance between neighbor ions is much bigger than the size of the $2s$ orbital, so that there is no confusion to which orbital an electron belongs. This is known as a "tight-binding limit". One can also consider the "nearly-free electron limit", which would be valid if the atomic orbitals spread over many lattice sites.

2. Tight-binding model

For our tight-binding model, we assume one orbital per atom, and these orbitals are taken to be orthogonal

$$\langle n|m\rangle = \int dx \phi_{2s}\left(x - R_n\right) \phi_{2s}\left(x - R_m\right) = \delta_{nm}. \tag{30}$$

This orthogonality is necessary in order to be able to associate creation and annihilation operators that satisfy the proper algebra to these states. The one dimensional tight-binding

Hamiltonian reads

$$\hat{H} = \epsilon \sum_{n,\sigma} c^{\dagger}_{n,\sigma} c_{n,\sigma} - t \sum_{n,\sigma} \left(c^{\dagger}_{n,\sigma} c_{n+1,\sigma} + h.c. \right) \tag{31}$$

the first term counts the on-site energy to have the electrons at any given site, and the second term describes hopping: if the electron is at site n, attraction from the neighboring ions can make it move either to $n+1$ or to $n-1$. This is known as nearest-neighbor hopping (nn hopping). Assuming a finite-size system (a finite number N of atoms), we have to be careful with is what happens at the ends of the chain. Here we impose the periodic boundary conditions (PBC), which state that if you move N sites along the chain, you get back to the original site. Mathematically, this means that$c^{\dagger}_{n+N,\sigma} = c^{\dagger}_{n,\sigma}$ for any n. Because of the PBC, the lattice is now translational invariant, and the Schrodinger equation in a periodic potential is guaranteed to have Bloch-type eigenfunctions

$$\phi(x + a) = \exp(ika)\phi(x) \tag{32}$$

Eq. (32) can be true only if

$$k = \frac{2\pi m}{Na} \qquad , \qquad m = -\frac{N}{2} + 1, \cdots, -1, 0, 1, \cdots, \frac{N}{2} \tag{33}$$

In this manuscript, we only consider the case when $m = 1$, such that $-\frac{\pi}{a} < k < \frac{\pi}{a}$, i.e. the first Brillouin zone. Now instead of dealing this problem in real space, we would prefer doing it in k-space. To do so, we can Fourier transform the creation and annihilation operators:

$$c^{\dagger}_{n,\sigma} = \sum_{k} \frac{\exp(-ikR_n)}{\sqrt{N}} c^{\dagger}_{k,\sigma} \qquad\qquad c_{n,\sigma} = \sum_{k} \frac{\exp(ikR_n)}{\sqrt{N}} c_{k,\sigma}$$

By pluggin these into Eq.(31), we could find that

$$\hat{H} = \sum_{k,\sigma} E(k) c^{\dagger}_{k,\sigma} c_{k,\sigma} \tag{34}$$

where $E(k) = \epsilon - 2t\cos(ka)$ is the dispersion relation which corresponds the one-electron eigenstate $c^{\dagger}_{k,\sigma} |0\rangle = \sum_{n=1}^{N} \frac{\exp(-ikna)}{\sqrt{N}} c^{\dagger}_{n,\sigma} |0\rangle$. Because the electrons are non-interacting, many-electron solutions are trivial as well: the eigenstate $c^{\dagger}_{k_1,\sigma_1} \cdots c^{\dagger}_{k_p,\sigma_p} |0\rangle$ has the eigenenergy $E(k_1) + \cdots + E(k_p)$, i.e. the sum of individual contributions. Back to the one dimensional chain of Li, in the ground-state they occupy the lowest available levels, from the lowest level ($k = 0$) to half of the Fermi level ($k = \pm\frac{\pi}{2a}$), to minimize the total energy, and we leave

empty the other half of the states, with energy $E(k) > \epsilon$. So clearly the total energy is lower than the $N\epsilon$ we would have if each Li kept its electron. The ground-state eigenstate is:

$$|GS\rangle = \prod_{-\frac{\pi}{2a} \leq k \leq \frac{\pi}{2a}} c^{\dagger}_{k,\sigma} |0\rangle \,, \tag{35}$$

and the ground-state energy is:

$$E_{GS} = \sum_{-\frac{\pi}{2a} \leq k \leq \frac{\pi}{2a}, \sigma} E(k) = N\epsilon - 4t \sum_{-\frac{\pi}{2a} \leq k \leq \frac{\pi}{2a}} \cos(ka) \tag{36}$$

3. Free electrons model

In this section, we first look at the free electron model, the Hamiltonian of free electron model reads:

$$\hat{H} = \sum_{k,\sigma} \epsilon_k c^{\dagger}_{k,\sigma} c_{k,\sigma}, \tag{37}$$

where $\epsilon_k = \frac{\hbar^2 k^2}{2m}$ is the kinetic energy of free electron.Again if we impose PBC, the condition for Eq.(32) to be true is if only $k = \frac{2\pi m}{L}$ so that $\exp(ikL) = 1$, which means, there is no restriction on the value on m.For the tight-binding chain, the restriction appeared because the values of the plane-waves only mattered at $R_n = na$. However, in this jellium model they matter at each $x \in [0, L]$, so each allowed valuegives a different, acceptable solution. Thus any integer m and so any $k = \frac{2\pi m}{L}$ is allowed. in other words there is no restriction to a Brillouin zone like before. If we have N electrons in this system, in the GS they will again occupy all states up to a k_F , so:

$$|GS\rangle = \prod_{|k|<k_F, \sigma} c^{\dagger}_{k,\sigma} |0\rangle \,, \tag{38}$$

and

$$E_{GS} = 2 \sum_{-|k|<k_F} \epsilon(k), \tag{39}$$

In the limit $L \to \infty$, we can replace the summation with integrals:$\sum_{k_1}^{k_2} f(k) = \frac{L}{2\pi} \int dk f(k)$.We then find:$k_F = \frac{\pi n}{2}$, where $n = N/L$ is the electron density, and we can then go and calculate the GS energy:

$$E_{GS} = \frac{N(\hbar \pi n)^2}{24m}. \tag{40}$$

The nearly free electron case is a modification of free electron model by including a weak potential well. We will not go any further into it before things get really messy.

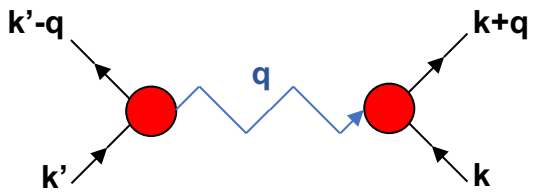

FIG. 1: (color online) Diagrammatic representation of the effective electron-electron interaction mediated by the exchange of a phonon (blue zigzag line). Black lines indicate electronic states. The red circle is the vertex

C. Electron-phonon interactions

So far, we considered the motion of electrons in the static periodic potential that would arise if the ions were frozen in their equilibrium positions. In this section, we are going to consider how the existence of phonons could affect the behavior of the valence electrons. The process involving the electron-phonon interaction is the scattering of a single electron by a simultaneous creation or annihilation of a single phonon, as diagrammatically shown in Fig. 1. The probability for the scattering process is called the electron-phonon vertex g. Assume the ion is located at position $\boldsymbol{R}_{n,\alpha}$, at a displacement $\boldsymbol{u}_{n,\alpha}$ from its equilibrium position $\boldsymbol{R}^{(0)}_{n,\alpha}$, such that

$$\boldsymbol{R}_{n,\alpha} = \boldsymbol{R}^{(0)}_{n,\alpha} + \boldsymbol{u}_{n,\alpha}. \tag{41}$$

If the potential of the ion is assumed to be rigid, the interaction energy of the electronic charge density with the ions in real space is simply:

$$\hat{V}_{el-ph} = \sum_{i,a} V(\boldsymbol{r} - \boldsymbol{R}_{i,a}) \tag{42}$$

Here, $V(\boldsymbol{r})$ is the screened potential similar to what we used in electron-electron and ion-ion interactions.For small amplitude vibrations, we can expand in powers of $\boldsymbol{u}_{n,\alpha}$:

$$\hat{V}_{el-ph} = \sum_{i=1}^{N}\sum_{n,\alpha} V(\boldsymbol{r} - \boldsymbol{R}_{i,a}) \approx \sum_{i=1}^{N}\sum_{n,\alpha} V(\boldsymbol{r} - \boldsymbol{R}^{(0)}_{n,a}) - \sum_{i=1}^{N}\sum_{n,\alpha} \boldsymbol{u}_{n,\alpha}\nabla_{\boldsymbol{R}_{n,\alpha}} V(\boldsymbol{r} - \boldsymbol{R}_{n,a}) \tag{43}$$

The first term in this equation is the interaction of the electrons with the static, frozen lattice that was already included in the electronic Hamiltonian, so we do not need to consider it again. The second term is the extra part describing the electron-phonon interaction.The

second quantization of the second term is:

$$\hat{V}_{el-ph} = -\sum_{\substack{b,\boldsymbol{k},\sigma \\ b',\boldsymbol{k}',\sigma'}} \langle b,k,\sigma|\cdots|b',k',\sigma'\rangle\, c^{\dagger}_{b,k,\sigma} c_{b',k',\sigma'} \tag{44}$$

where b is the band index, and

$$\langle b,k,\sigma|\cdots|b',k',\sigma'\rangle = \int d\boldsymbol{r}\phi^{*}_{bk\sigma}(\boldsymbol{r}) \sum_{n,\alpha} \boldsymbol{u}_{n,\alpha} \nabla V_{\alpha}(\boldsymbol{r}-\boldsymbol{R}_{n,\alpha}) \phi_{b'k'\sigma'}(\boldsymbol{r}). \tag{45}$$

Now, In order to do the integral in Eq.(45), we rewrite $\phi_{bk\sigma}(\boldsymbol{r}$ in term of Bloch state:

$$\phi_{bk\sigma}(\boldsymbol{r}) = \frac{\exp(i\boldsymbol{k}\boldsymbol{r})}{\sqrt{V}} u_{b\boldsymbol{k}}(\boldsymbol{r})\chi(\sigma). \tag{46}$$

Also, the second quantization of $\boldsymbol{u}_{n,\alpha}$ read,

$$\boldsymbol{u}_{n,\alpha} = \sum_{j,\boldsymbol{q}} \sqrt{\frac{\hbar}{2M_{\alpha}\omega_j(\boldsymbol{q})}} \boldsymbol{e}^{(j)}_{\alpha}(\boldsymbol{q}) \cdot \frac{\exp(i\boldsymbol{q}\cdot\boldsymbol{R}_n)}{\sqrt{N}} \left(b_{j,\boldsymbol{q}} + b^{\dagger}_{j,-\boldsymbol{q}}\right). \tag{47}$$

Here $\boldsymbol{e}^{(j)}_{\alpha}(\boldsymbol{q})$ is the eigenvector corresponds to N allowed $\boldsymbol{q}$, with frequencies $\omega_j(\boldsymbol{q})$, $j = 1,\cdots,3r$ (i.e. size of the dynamical matrix of phonon). After doing all the math, we find that the electron-phonon interaction has the general form:

$$\hat{V}_{el-ph} = \frac{1}{\sqrt{N}} \sum_{\boldsymbol{k},\boldsymbol{q},\sigma} g(\boldsymbol{k},\boldsymbol{q})(b^{\dagger}_{-\boldsymbol{q}} + b_{\boldsymbol{q}}) c^{\dagger}_{\boldsymbol{k}+\boldsymbol{q},\sigma} c_{\boldsymbol{k},\sigma} \tag{48}$$

where the vertex $g(\boldsymbol{k},\boldsymbol{q})$ contains all the multiplying constant.

1. The Fröhlich Hamiltonian

The Fröhlich Hamiltonian describes free electrons (no underlying lattice, i.e. a jellium model) coupled to the longitudinal acoustic phonons through unscreened Coulomb interactions:

$$\hat{H} = \sum_{\boldsymbol{k},\sigma} \epsilon(\boldsymbol{k}) c^{\dagger}_{\boldsymbol{k},\sigma} c_{\boldsymbol{k},\sigma} + \sum_{\boldsymbol{q}} \hbar\omega_{\boldsymbol{q}} b^{\dagger}_{\boldsymbol{q}} b_{\boldsymbol{q}} + \frac{1}{\sqrt{N}} \sum_{\boldsymbol{k},\boldsymbol{q}} M(q)(b^{\dagger}_{-\boldsymbol{q}} + b_{\boldsymbol{q}}) c^{\dagger}_{\boldsymbol{k}+\boldsymbol{q},\sigma} c_{\boldsymbol{k},\sigma'} \tag{49}$$

where the vertex turns out to be

$$M(q) = \sqrt{\frac{\hbar}{2M\omega_{\boldsymbol{q}}}} q V(q)$$

This general form of the Frohlich Hamiltonian will be a good starting point for the green's function and many-body perturbation for the discussion of electron-phonon coupling effects in periodic solids.

2. The Hubbard-Holstein Hamiltonian

The Hubbard-Holstein hamiltonian is the simplest model one can write. By assuming the valence electrons are coupling to a single branch of optical phonons, which are described by Einstein model, the Hamiltonian reads:

$$\hat{H} = -\sum_{n,m,\sigma} t_{n,m} c^{\dagger}_{n,\sigma} c_{m,\sigma} + \hbar\Omega \sum_{n} b^{\dagger}_{n} b_{n} + g \sum_{n,\sigma} c^{\dagger}_{n,\sigma} c_{n,\sigma} (b^{\dagger}_{n} + b_{n}) \tag{50}$$

The first term describes the hopping of the electrons on the lattice (usually restricted to nearestneighbor hopping only); the second is the phonons and the third is the Holstein coupling. Even this model, which is as simple as one can write, cannot be solved exactly except when either $t = 0$ (no hopping) or $g = 0$ (no coupling).

3. The Peierls/SSH Hamitonian

We study a simple cubic lattice with Peierls-type electron phonon coupling, arising from the modulation of the hopping integral between neighbor sites as the distance between them varies. Our starting point is a 3D generalization of the 1D Su-Schrieffer-Heeger (SSH) model, but with optical phonons:

$$\hat{H} = \hat{H}_{el} + \hat{H}_{ph} + \hat{V}_{el-ph}, \tag{51}$$

where

$$\hat{H}_{el} = -t \sum_{\langle i,j \rangle, \sigma} (c^{\dagger}_{i,\sigma} c_{j,\sigma} + H.c.) - \mu \sum_{i} \hat{n}_{i} \tag{52}$$

describes nearest neighbor (nn) hopping, μ is the chemical potential and $\hat{n}_i = \sum_\sigma c^{\dagger}_{i,\sigma} c_{i,\sigma}$. The next term describes three independent Einstein modes for oscillations of the lattice sites along the $\gamma = \{x, y, z\}$ axes: $\hat{H}_{ph} = \Omega \sum_{i,\gamma} b^{\dagger}_{i,\gamma} b_{i,\gamma}$, where $b^{\dagger}_{i,\gamma}$ creates a γ-mode phonon at site i and $\hbar = 1$. Finally,

$$\hat{V}_{el-ph} = g \sum_{i,\sigma,\gamma} (c^{\dagger}_{i,\sigma} c_{i+\boldsymbol{\gamma},\sigma} + H.c.)(b^{\dagger}_{i+\boldsymbol{\gamma},\gamma} + b_{i+\boldsymbol{\gamma},\gamma} - b^{\dagger}_{i,\gamma} - b_{i,\gamma}) \tag{53}$$

is the Peierls electron-phonon coupling [17–20]. We use the short-hand notation $i \pm \boldsymbol{x}$ for the site located at $\boldsymbol{R}_i \pm \boldsymbol{x}$, etc., with the lattice constant set to $a = 1$.

We use the dimensionless parameter $\lambda = 2g^2/(\Omega t)$ to characterize the strength of the electron-phonon coupling. This is identical to the 1D definition [23] because the tripling

of the free electron bandwidth in 3D is compensated for by the existence of three phonon modes. However, we emphasize that within the approximations used below, a carrier only couples to one phonon mode at a time, so $\lambda/3$ might be a more appropriate measure of the electron-phonon coupling strength.

In the anti-adiabatic limit $\Omega \gg t, g$, we integrate out the high-energy manifolds with one or more phonons. For a system with just two electrons of opposite spin, this leads to an effective low-energy Hamiltonian which is a direct generalization of that obtained in 1D [24]:

$$\hat{\mathcal{H}} = \hat{T}_{\text{eff}} + \hat{U}_{\text{eff}} + \mathcal{O}\left(\frac{1}{\Omega^2}\right) \tag{54}$$

where the single-polaron part

$$\hat{T}_{\text{eff}} = \hat{H}_{el} + \epsilon_0 \sum_i \hat{n}_i + t_3 \sum_{i,\gamma,\sigma} (c^\dagger_{i,\sigma} c_{i+2\boldsymbol{\gamma},\sigma} + H.c.) \tag{55}$$

now includes the polaron formation energy $\epsilon_0 = -12g^2/\Omega$, while the bare nn hopping is supplemented by the phonon-mediated, 3^{rd} nn hopping with $t_3 = g^2/\Omega$. Note that 2^{nd} nn hoping cannot arise from emission and absorption of one phonon, because hopping along different axes is modulated by different phonons; such processes can arise only at higher order.

The effective, phonon-mediated interaction between polarons is given by $\hat{U}_{\text{eff}} = \hat{U}_{0,2} + \hat{U}_1$ [24], where

$$\begin{aligned} \hat{U}_{0,2} = &-T_0 \sum_{i,\gamma} [c^\dagger_{i-\boldsymbol{\gamma},\uparrow} c^\dagger_{i-\boldsymbol{\gamma},\downarrow} c_{i,\downarrow} c_{i,\uparrow} + H.c.] \\ &+ T_2 \sum_{i,\gamma} [(c^\dagger_{i+\boldsymbol{\gamma},\uparrow} c^\dagger_{i-\boldsymbol{\gamma},\downarrow} - c^\dagger_{i+\boldsymbol{\gamma},\downarrow} c^\dagger_{i-\boldsymbol{\gamma},\uparrow}) c_{i,\downarrow} c_{i,\uparrow} + H.c.] \end{aligned} \tag{56}$$

describes nn pair hopping of an on-site pair, with $T_0 = 4g^2/\Omega$, and hybridization between an on-site and a 3^{rd} nn singlet pair, with $T_2 = 2g^2/\Omega$, respectively, while

$$\begin{aligned} \hat{U}_1 = &T_1 \sum_{i,\gamma,\sigma} [c^\dagger_{i+\boldsymbol{\gamma},\sigma} c^\dagger_{i+2\boldsymbol{\gamma},-\sigma} c_{i+\boldsymbol{\gamma},-\sigma} c_{i,\sigma} + H.c.] \\ &- J \sum_{i,\gamma,\sigma} c^\dagger_{i+\boldsymbol{\gamma},\sigma} c^\dagger_{i,-\sigma} c_{i+\boldsymbol{\gamma},-\sigma} c_{i,\sigma} \end{aligned} , \tag{57}$$

describes directional (parallel to its backbone) pair hopping of a nn singlet pair, with $T_1 = 2g^2/\Omega$, and a nn antiferromagnetic exchange with $J = 4g^2/\Omega$, respectively.

The unusual form of this effective interaction is a direct consequence of the $g(\boldsymbol{k}, \boldsymbol{q})$ nature of the Peierls electron-phonon coupling. $\hat{U}_{\text{eff}}$ is attractive because polarons can lower their kinetic energy if they are bound into singlet bipolarons that move together. This is opposite to the density-density effective interactions mediated through phonon coupling of $g(\boldsymbol{q})$ type, which favor static bipolarons; further discussion can be found in Ref. 24.

Hereafter, this two-polaron Hamiltonian (corresponding to zero density for an infinite lattice) is assumed to be a good model for systems with low but finite carrier concentrations. This is because even though the phonon-induced renormalization of the quasiparticle dispersion and of their effective interactions also depend on the carrier concentration, in the limit of very low concentrations their values must be close to those obtained in the zero-concentration limit. Furthermore, as we show below, small quantitative changes in the values of these effective parameters do not affect our conclusions.

D. The BCS Theory of Superconductivity

Superconductivity (SC) is one of the most well known macroscopic quantum effects that have emerged in condensed matter physics. It was discovered in 1911 by K. Onnes, who found out that the resistence of mercury suddenly dropped to zero at $4.2K$. The temperature below which a metal becomes superconducting is called the critical temperature(T_c). In "conventional superconductors", which we understand and this is usually from a few K up to 20-30K. More recently, classes of so-called high-temperature superconductors have been discovered, notably the cuprates in late 1980s by Bednorz and Müller and iron-based superconductors around 2008. To date, the highest confirmed critical temperature for a superconducting transition, have some $T_c = 135$ K at room pressure and approximately 250 K under when applying high pressure. These new discovery broke all constraints on the maximum T_c predicted by the conventional theory of low-temperature superconducting metals and their alloys. These "unconventional superconductors" are not yet understood. They share many basic properties with the conventional ones, but the mechanism reponsible for superconductivity is (almost certainly) not the same. The details standard Bardeen-Cooper-Schrieffer (BCS) model can be found in [2], which is the first and simplest generic model that explains conventional SC, since its discovery.

1. The BCS Hamiltonian

The BCS superconductivity starts with the Frölich Hamiltonian, with an observation of electrons could attract each other and degenerate into a pair, called Cooper's pair, due to their interaction with the vibrating atoms in crystal lattice. Due the Pauli's principle of exclusion, the electrons tend to pair into triplet, with zero average momentum in the pair. For these reason, BCS introduced a reduced Hamiltonian involves only $(\boldsymbol{k},\uparrow,-\boldsymbol{k},\downarrow)$. The general form of the BCS Hamiltonian reads:

$$\hat{\mathcal{H}}_{BCS} = \sum_{\boldsymbol{k}} \xi_{\boldsymbol{k}} c^{\dagger}_{\boldsymbol{k},\sigma} c_{\boldsymbol{k},\sigma} + \sum_{\boldsymbol{k},\boldsymbol{k}'} c^{\dagger}_{\boldsymbol{k},\uparrow} c^{\dagger}_{-\boldsymbol{k},\downarrow} \Delta_{\boldsymbol{k}}, \tag{58}$$

where

$$\Delta(\boldsymbol{k}) = \sum_{\boldsymbol{k}'} V_{k,k'} c_{-\boldsymbol{k}',\downarrow} c_{\boldsymbol{k}',\uparrow}. \tag{59}$$

The first term $\xi = \epsilon_{\boldsymbol{k}} - \mu$ is the band energy dispersion referred to the chemical potential μ. The second term is the attractive potential where we have $V_{k,k'} = -V_0$ within the Debye frequency ($\hbar\omega_D$) of the Fermi surface, and zero elsewhere. Because V_0 is small, we can treat this Hamiltonian in Hatree-Fock approximation. We first perform the Bogoliubov-Valatin transformation to Eq.(58). With a new set of operators:

$$\begin{pmatrix} \gamma_{\boldsymbol{k}\uparrow} \\ \gamma^{\dagger}_{-\boldsymbol{k}\downarrow} \end{pmatrix} = \begin{pmatrix} u_{\boldsymbol{k}} & -v_{\boldsymbol{k}} \\ v_{\boldsymbol{k}} & u_{\boldsymbol{k}} \end{pmatrix} \begin{pmatrix} c_{\boldsymbol{k}\uparrow} \\ c^{\dagger}_{-\boldsymbol{k}\downarrow} \end{pmatrix}, \tag{60}$$

and $|u_k|^2 + |v_k|^2 = 1$, we can rewrite $c^{\dagger}_{\boldsymbol{k},\uparrow} c^{\dagger}_{-\boldsymbol{k},\downarrow}$ in terms of $\gamma^{\dagger}_{\boldsymbol{k}\uparrow}, \gamma^{\dagger}_{-\boldsymbol{k}\downarrow}$. Then we substitute them into Eq.(60), and choose

$$u^2_{\boldsymbol{k}} = \frac{1}{2}\left(1 + \frac{\xi_{\boldsymbol{k}}}{E_{\boldsymbol{k}}}\right) \qquad v^2_{\boldsymbol{k}} = \frac{1}{2}\left(1 - \frac{\xi_{\boldsymbol{k}}}{E_{\boldsymbol{k}}}\right).$$

After doing some rearrangement, the resulting equation is

$$\hat{\mathcal{H}}_{BCS} \approx E_{GS} + \sum_{\boldsymbol{k},\sigma} E_{\boldsymbol{k}} \gamma^{\dagger}_{\boldsymbol{k},\sigma} \gamma_{\boldsymbol{k},\sigma}. \tag{61}$$

where $E_{\boldsymbol{k}} = \sqrt{\xi^2_{\boldsymbol{k}} + |\Delta_{\boldsymbol{k}}|^2}$.This transformation reduces the whole problem of correlated electrons to an ideal Fermi gas comprising two types of new non-interacting fermions, and the transformed Hamiltonian becomes diagonal. Finally , the value of order parameter $\Delta_{\boldsymbol{k}}$ is determined from the self-consistent equation:

$$\Delta_{\boldsymbol{k}} = -\frac{1}{2V} \sum_{\boldsymbol{k}'} V_{k,k'} \frac{\Delta'_{\boldsymbol{k}}}{\sqrt{\xi^2_{\boldsymbol{k}} + |\Delta_{\boldsymbol{k}'}|^2}} \tanh\left[\frac{\beta E_{\boldsymbol{k}'}}{2}\right]. \tag{62}$$

which is also called the gap equation. To find the critical temperature T_C,there is a simple universal relation between the $T = 0$ gap and T_C for all weakly coupled BCS superconductors:

$$2\Delta = 3.52 k_B T_C. \tag{63}$$

III. METHODS

In this section, we show how we incorporate the three dimensional $\hat{U}_{\text{eff}}$ we found in previous section into the BCS model. The effect of this unusual $\hat{U}_{\text{eff}}$ pair-hopping effective attraction on SC was not analyzed before, to the best of our knowledge. We do this in the most straigthforward way: we switch to momentum space and keep in the interaction only terms scattering pairs of polarons between $(\boldsymbol{k}\uparrow, -\boldsymbol{k}\downarrow)$ states, as done in the standard BCS approach [2]. This reduces the Hamiltonian of Eq. 54 to:

$$\mathcal{H}_{SC} = \sum_{\boldsymbol{k},\sigma} \xi_{\boldsymbol{k}} c^\dagger_{\boldsymbol{k}\sigma} c_{\boldsymbol{k}\sigma} + \sum_{k,k'} \frac{U_{\text{eff}}(\boldsymbol{k},\boldsymbol{k'})}{N^3} c^\dagger_{\boldsymbol{k}\uparrow} c^\dagger_{-\boldsymbol{k}\downarrow} c_{-\boldsymbol{k'}\downarrow} c_{\boldsymbol{k'}\uparrow}$$

where $N^3 \to \infty$ is the number of lattice sites, $\xi_{\boldsymbol{k}} = \epsilon_{\boldsymbol{k}} - \mu$ is the single polaron dispersion

$$\epsilon_{\boldsymbol{k}} = \epsilon_0 - 2t \sum_\gamma \cos(k_\gamma) + 2t_3 \sum_\gamma \cos(2k_\gamma) \tag{64}$$

measured from the Fermi energy, and the scattering vertex for pairs with $\boldsymbol{k}_{tot} = 0$ is:

$$\begin{aligned} U_{\text{eff}}(\boldsymbol{k},\boldsymbol{k'}) = -6T_0 + 2T_2 \sum_\gamma \Big[\cos(2k_\gamma) + \cos\big(2k'_\gamma\big) \Big] \\ + 4T_1 \sum_\gamma \cos\big(k_\gamma - k'_\gamma\big) - 2J \sum_\gamma \cos\big(k_\gamma + k'_\gamma\big). \end{aligned}$$

Note that this vertex depends not just on $\boldsymbol{k} - \boldsymbol{k'}$ like for regular, density-density interactions, but also on $\boldsymbol{k} + \boldsymbol{k'}$. This is a direct consequence of the pair-hopping terms.

Again, we use the Bogoliubov-Valatin transformation to find the usual mean-field approximation: $\mathcal{H}_{SC} \approx E_{GS} + \sum_{\boldsymbol{k}\sigma} E_{\boldsymbol{k}} \gamma^\dagger_{\boldsymbol{k}\sigma} \gamma_{\boldsymbol{k}\sigma}$, where the quasiparticle energies are $E_{\boldsymbol{k}} = \sqrt{\xi^2_{\boldsymbol{k}} + \Delta^2_{\boldsymbol{k}}}$ and the SC gap is given by the standard gap equation:

$$\Delta_{\boldsymbol{k}} = -\frac{1}{2N^3} \sum_{\boldsymbol{k'}} \frac{U_{\text{eff}}(\boldsymbol{k},\boldsymbol{k'}) \Delta_{\boldsymbol{k'}}}{E_{\boldsymbol{k'}}} \tanh \frac{E_{\boldsymbol{k'}}}{2kT}. \tag{65}$$

The chemical potential fixes the $T = 0$ carrier concentration:

$$n = \frac{2}{N^3} \sum_{\boldsymbol{k}} |v_{\boldsymbol{k}}|^2 = \frac{1}{N^3} \sum_{\boldsymbol{k}} \left[1 - \frac{\xi_{\boldsymbol{k}}}{E_{\boldsymbol{k}}} \right]. \tag{66}$$

For our $U_{\rm eff}(\boldsymbol{k},\boldsymbol{k'})$, the SC gap has the general form:

$$\Delta_{\boldsymbol{k}} = \Delta_s + \Delta_{s^*}\sum_\gamma \cos(2k_\gamma) + \Delta_p \sum_\gamma \sin(k_\gamma) \tag{67}$$

where

$$\begin{aligned}
\Delta_s &= \frac{1}{N^3}\sum\nolimits_{\boldsymbol{k'},\gamma}\Big[T_0 - T_2\cos\big(2k'_\gamma\big)\Big]\frac{\Delta_{\boldsymbol{k'}}}{E_{\boldsymbol{k'}}}\tanh\frac{E_{\boldsymbol{k'}}}{2kT}\\
\Delta_{s^*} &= -\frac{T_2}{N^3}\sum\nolimits_{\boldsymbol{k'}}\frac{\Delta_{\boldsymbol{k'}}}{E_{\boldsymbol{k'}}}\tanh\frac{E_{\boldsymbol{k'}}}{2kT}\\
\Delta_p &= -\frac{2T_1+J}{N^3}\sum\nolimits_{\boldsymbol{k'},\gamma}\sin k'_\gamma\frac{\Delta_{\boldsymbol{k'}}}{E_{\boldsymbol{k'}}}\tanh\frac{E_{\boldsymbol{k'}}}{2kT}
\end{aligned} \tag{68}$$

We note that another term with extended s^* symmetry, $\propto \sum_\gamma \cos k_\gamma$, vanishes because its prefactor $2T_1 - J = 0$, however it could contribute to $\Delta_{\boldsymbol{k}}$ if higher order terms further renormalize the values of T_1 and J.

We solved these equations iteratively on a lattice with $N^3 = 30^3$ sites, with an accuracy below $10^{-6}t$, for values of μ near the bottom of the polaron band so that the average carrier concentration $n < 0.20$ is small. As expected, we find that s and p symmetries do not co-exist, and moreover, $\Delta_p = 0$ because of the overall minus sign in its gap equation (68); we comment more on this symmetry below. Thus, the SC gap has $s + s^*$ contributions.

IV. RESULTS

We begin at $T = 0$. For small λ we find no SC for small carrier concentrations $n \to 0$: both Δ_s and Δ_{s^*} vanish. This does not contradict the BCS theory, which is valid in the limit $E_F \gg \Omega, \lambda \ll 1$. In that case, the phonon-mediated scattering –within an energy shell of width Ω from the Fermi surface– is effectively a 2D problem and bound solutions (Cooper pairs) form for arbitrarily weak attractive interactions. Our calculation, however, is in the opposite limit $\Omega \gg E_F$ where the scattering is 3D and a bound solution is expected only if the attractive potential is strong enough.

As we increase λ, we find finite Δ_s, Δ_{s^*} if $n \geq n_c$ becomes large enough. This is shown in Fig. 2(i), where for $\lambda = 0.5$ we plot the evolution of Δ_s and Δ_{s^*} (left-hand vertical axis) with μ; superimposed is the evolution of n (right-hand vertical axis) with μ. When μ is at the bottom of the polaron band so that $n \to 0$, the gaps vanish. However, for $n > n_c \approx 0.07$, SC appears and the magnitudes of Δ_s and Δ_{s^*} increase fast with n. The value of n_c decreases

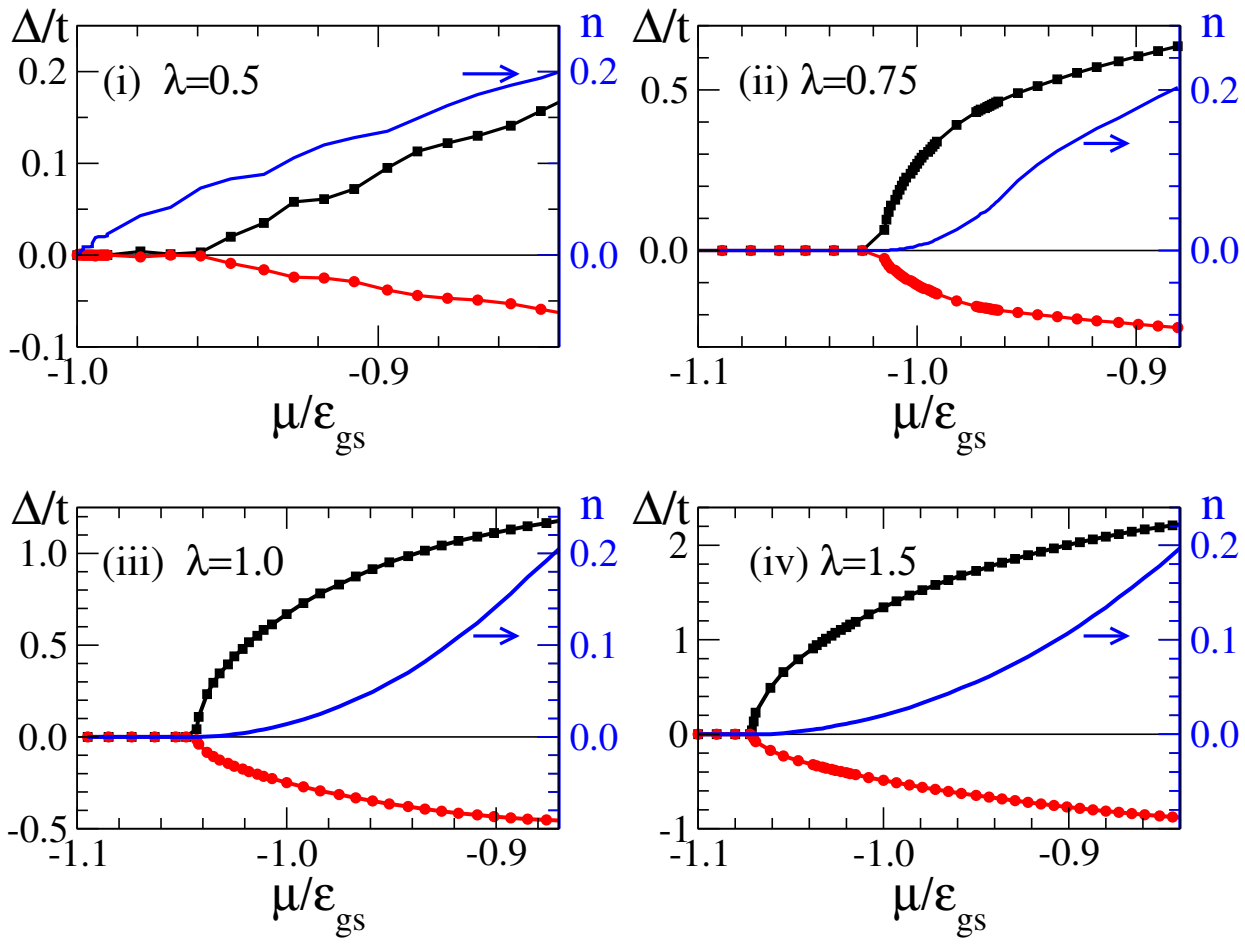

FIG. 2: (color online) Magnitudes of the superconducting gaps Δ_s/t (black squares) and Δ_{s^*}/t (red circles) vs. μ/ϵ_{gs}, where ϵ_{gs} is the corresponding polaron GS energy. The blue full line shows the average carrier concentration n (right-side scale). Panels correspond to effective couplings $\lambda = 0.5, 0.75, 1.0$ and 1.5, respectively.

with increasing λ. We do not try to pinpoint it here because even for $\lambda = 0.5$ there are still finite N size effects (small oscillations) in the results, and these become worse as λ decreases. Moreover, our focus here is on larger λ, where $n_c \to 0$, as we show next. For reference, we mention that for $\lambda = 0.25$, we find $n_c \sim 0.2$, which is probably above the low carrier concentrations for which our model is quantitatively accurate.

Panels (ii)-(iv) of Fig. 2 show the same results for $\lambda = 0.75, 1.0, 1.5$, respectively. Here we find robust values for Δ_s and Δ_{s^*} at all $n \geq n_c = 0$. For a fixed λ, the magnitudes of the gaps increase monotonically with n. At a fixed n, they increase fast with λ so that for $\lambda \sim 1$, both Δ_s and Δ_{s^*} are of order t, which is an *extremely large* energy scale for SC.

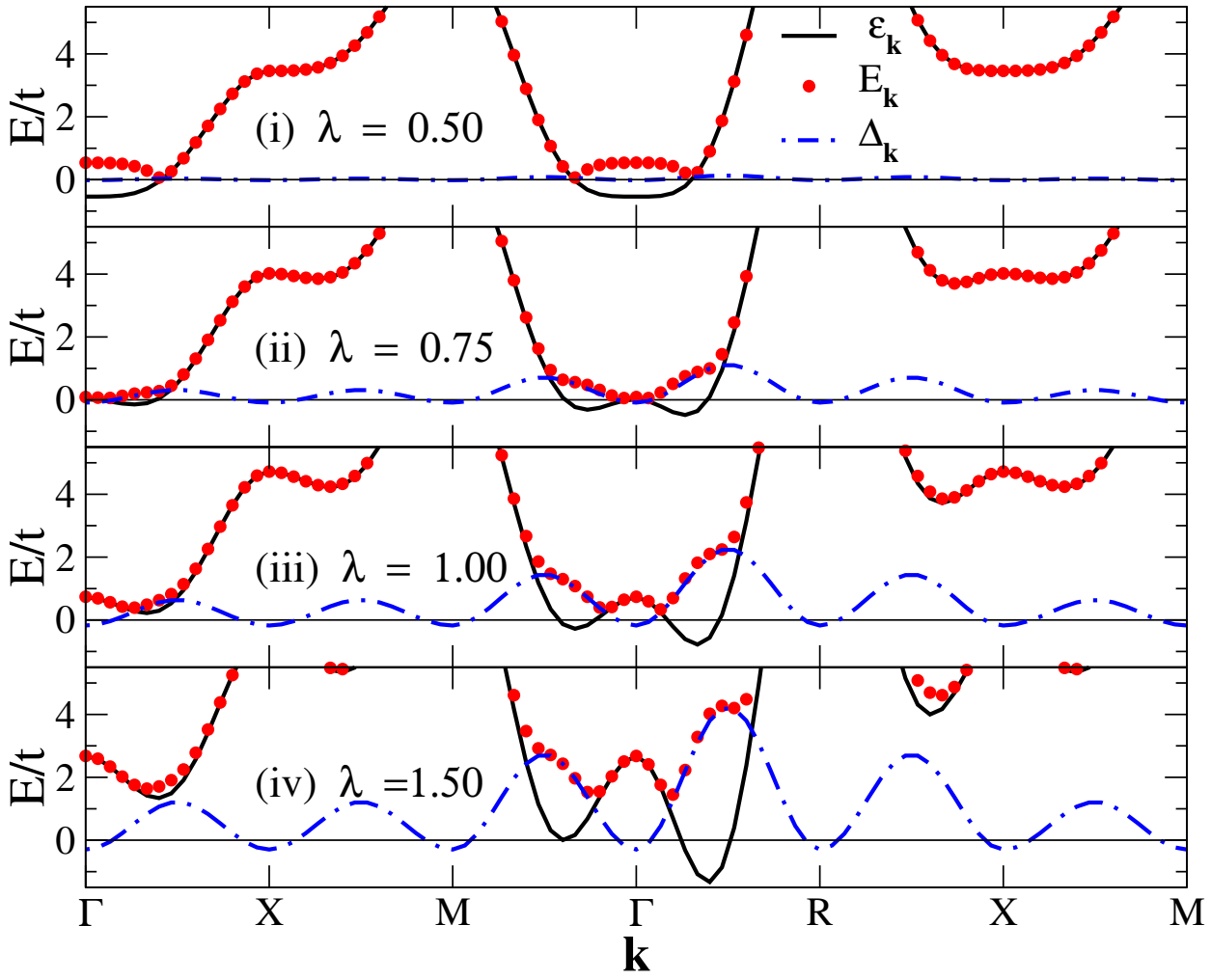

FIG. 3: (color online) Polaron energy $\epsilon_{\boldsymbol{k}}$ (solid black line), quasiparticle energy $E_{\boldsymbol{k}}$ (red circles) and SC gap $\Delta_{\boldsymbol{k}}$ (dot-dashed blue line) along high-symmetry lines in the Brillouin zone. All energies are in units of t, and μ is chosen such that $n = 0.1$ for all values $\lambda = 0.5, 0.75, 1.0, 1.5$ shown in panels (i)-(iv), respectively.

To clarify the origin of this unusual behavior, in Fig. 3 we plot the polaron dispersion $\epsilon_{\boldsymbol{k}} = \xi_{\boldsymbol{k}} + \mu$, the quasiparticle energy $E_{\boldsymbol{k}}$ and the gap $\Delta_{\boldsymbol{k}}$ along various lines in the Brillouin zone. The chemical potential is chosen such that $n = 0.1$. Consider first the evolution of $\epsilon_{\boldsymbol{k}}$ with λ: for $\lambda < 0.5$, the polaron ground state is at the Γ point, however for $\lambda > 0.5$ there are 8 degenerate ground-states at finite momentum $\pm\boldsymbol{k}_{gs}$ lying along the $\Gamma - R$ line and its symmetric counterparts. This is because at small λ the polaron dispersion is dominated by the nn hopping t term that favors a GS at the Γ point, while for $\lambda \geq 0.5$, the polaron dispersion is dominated by the 3^{rd} nn hoping term t_3, which favors a GS at the R point [23].

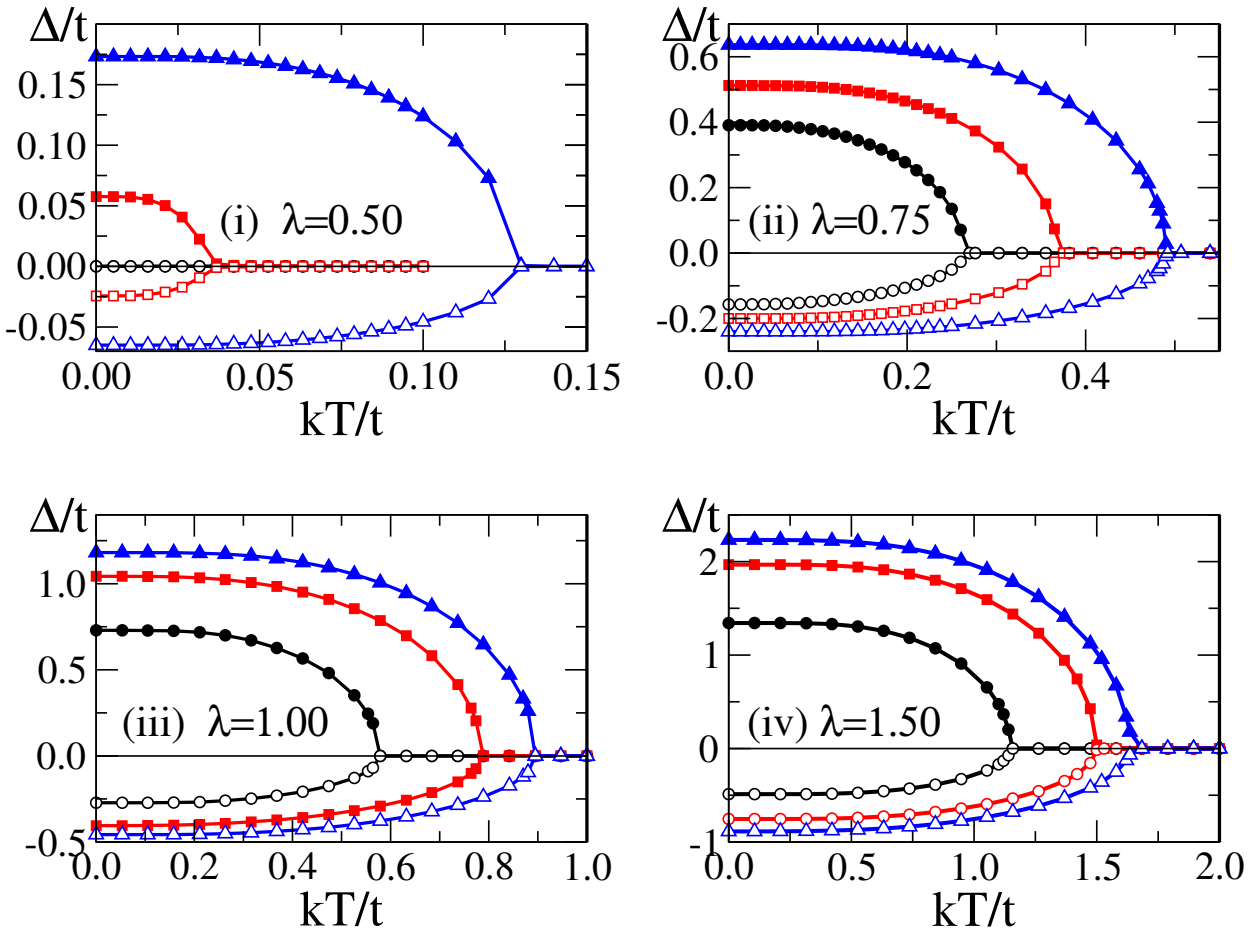

FIG. 4: (color online) Superconducting gaps Δ_s/t (full symbols) and Δ_{s^*}/t (empty symbols) vs. kT/t. The three sets of lines correspond to $n = 0.05$ (black circles), 0.10 (red squares) and 0.20 (blue triangles), respectively.

As a result, for μ near the bottom of the band, the system evolves from having a single, quasi-spherical Fermi sea when λ is small, to having eight Fermi pockets when λ is larger (these become connected if μ is further increased).

This significant change in the polaron dispersion results in the very different nature of the SC gap at small λ vs. large λ: in panel (i) we see a BCS-like picture, with a tiny and nearly constant gap opening at the Fermi energy. As λ increases, so does the gap magnitude. Because of the opposite signs of Δ_s and Δ_{s^*}, the gap is negative near the Γ point but switches sign and becomes positive and is maximum on the "outer" side of the Fermi pockets, on the $\Gamma - R$ lines. For $\lambda = 0.75$ and this μ, the smallest gap magnitude is close to the Γ point, on the "inner" side of the Fermi pockets, and its sign is negative, whereas the "outer" side

has a significant, positive gap. This shows that by adjusting the parameters, one can find an unconventional gap that closes on the Fermi pocket surface. The more typical behavior is found for larger μ and/or λ, with the Fermi pockets significantly gapped, the gap being positive. Interestingly, we see that the gap is considerable also in the regions lying between two Fermi pockets, on the $\Gamma - M$ and $\Gamma - X$ lines, even when these regions lie well above μ in the absence of SC.

The results in Fig. 3 suggest that the SC gap is considerable at $T = 0$ even for this rather low carrier concentration $n = 0.1$ if $\lambda > 0.5$. This is demonstrated more clearly in Fig. 4 where we plot Δ_s (full symbols) and Δ_{s^*} (empty symbols) vs. temperature for three carrier concentrations $n = 0.05$ (circles), 0.1 (squares) and 0.2 (triangles). For $\lambda = 0.5$ there is no SC for $\langle n \rangle = 0.05$, and T_C for larger n is rather small (although if t is in the hundred meV range, such T_C would be high). For larger λ we see a significant $kT_C \sim t$ even for $n = 0.05$, suggesting that even narrow-band materials with a t of tens of meV could sustain room temperature SC.

V. DISCUSSION

The fact that for larger λ we find SC to occur for all carrier concentrations shows that it has BEC nature. The key ingredient is the attractive $U_{\rm eff}(\boldsymbol{k}, \boldsymbol{k}')$ that strongly binds very light bipolarons at all λ, so that both the pair binding energy and their coherence energy are large. Bipolarons are light because $U_{\rm eff}$ promotes their mobility, by acting on pairs of carriers that hop together. This is a direct consequence of the $g(\boldsymbol{k}, \boldsymbol{q})$ electron-phonon coupling. In 1D stable bipolarons form for any λ [24]; in 3D there is a finite threshold for binding, hence different behaviour at small vs. large λ.

Regarding our methodology, we emphasize that these results are in the antiadiabatic limit $\Omega/t \to \infty$ simply because this is where we can obtain the analytical form of the effective polaron Hamiltonian (54), which allows us to carry out the calculations relatively easily. In 1D, the bipolaron behavior remains qualitatively similar down to $\Omega \sim 0.5t$ [25], and we expect the same in 3D (what happens in the adiabatic limit $\Omega/t \to 0$ is not yet clear). Similarly, we use the BCS variational solution because of its simplicity. It may overestimate T_C like is typical for mean-field methods, however the predicted values are so large that this work should provide a strong motivation for the implementation of costly numerical

methods to study these results more accurately.

Beside the high-T_C values, another very exciting result is the possibility of p-wave SC. It does not occur within these approximations because of the lack of a p^* term to combine with the p term of Eq. 68 the way the s and s^* terms do. A p^* term may arise in a more accurate treatment and/or for different $g(\boldsymbol{k}, \boldsymbol{q})$ couplings. Studying such possibilities opens another important new area, given the need for p-type SC in the topological context.

VI. CONCLUSION

In this work, we proposed a proof-of-theory that high-T_c, unconventional SC is possible within the phonon glue framework. We have found superconductivity with very high critical temperatures occurs at all carrier concentrations if the electron-phonon coupling is not too weak, with a gap of $s + s^*$ symmetry that closes on the Fermi surface for appropriate parameters. The possibility of finding the elusive p-type superconductivity is also revealed, although this is not stable within the approximations we use. The last question is for which materials could this apply. Our work is a proof-of-principle that exciting physics appears in the "anti"-Migdal limit, and a call for further studies. However, it is interesting to note that both doped $SrTiO_3$ and $BaBiO_3$ have "high"-T_C SC, believed to originate from $g(\boldsymbol{k}, \boldsymbol{q})$ electron-phonon couplings [26].

VII. ACKNOWLEDGEMENT

We thank Steve Johnston and Marcel Franz for useful discussions. This work was supported by JSPS KAKENHI Grant Number JP19K05371, by the Stewart Blusson Quantum Matter Institute (SBQMI) and by the Natural Sciences and Engineering Research Council of Canada (NSERC).

---

[1] H. Kamerlingh Onnes, Commun. Phys. Lab. Univ. Leiden. Suppl. **29** (1911).

[2] J. Bardeen, L. N. Cooper, and J. R. Schrieffer, Phys. Rev. 106, 162 (1957).

[3] M. L. Cohen and P. W. Anderson, AIP Conf. Proc. 4, 17-27 (1972).

[4] see, for example, I. Esterlis, S. A. Kivelson and D. J. Scalapino, njp Quantum Materials 3, 59 (2018) and references therein.

[5] W. A. Little, Phys. Rev. 134, A1416 (1964).

[6] D. Allender, J. Bray, and J. Bardeen, Phys. Rev. B 7, 1020 (1973).

[7] J. E. Hirsch and F. Marsiglio, Phys. Rev. B 39, 11515 (1989); *ibid*, Physica C 162-164, 591 (1989).

[8] F. Marsiglio and J. E. Hirsch, Physica C 468, 1047 (2008).

[9] J. G. Bednorz and K. A. Müller, Z. Phys. B: Condens. Matter 64, 189 (1986); J. G. Bednorz and K. A. Müller, Rev. Mod. Phys. **60**, 585 (1988).

[10] Y. Kamihara, H. Hiramatsu, M. Hirano, R. Kawamura, H. Yanagi, T. Kamiya, and H. Hosono, J. Am. Chem. Soc. 128, 10012 (2006).

[11] A. P. Mackenzie and Y. Maeno, Rev. Mod. Phys. **75**, 657 (2003); Y. Maeno, S. Kittaka, T. Nomura, S. Yonezawa, and K. Ishida, J. Phys. Soc. Jpn. **81**, 011009 (2012).

[12] G. R. Stewart Rev. Mod. Phys. **56**, 755 (1984); B.D. White, J.D. Thompson, M.B. Maple, Physica C **514**, 246 (2015).

[13] A. W. Sleight, J. L. Gillson and P. E. Bierstedt, Solid St. Commun. **17**, 27 (1975); R. J. Cava, B. Batlogg, J. J. Krajewski, R. Farrow, L. W. Rupp Jr, A. E. White, K. Short, W. F. Peck and T. Kometani, Nature **332**, 814–816 (1988); A. I. Golovashkin, A. V. Gudenko, L. N. Zherikhina, A. M. Tskhrovrebov, and M. L. Norton, J. Exp. Theor. Phys. **79**, 163 (1994); M. Braden, W. Reichardt, A. S. Ivanov, and A. Y. Rumiantsev, Europhys Lett. **34**, 531 (1996); D. Varshney, S. Shah, and R. K. Singh, Superlattices Microstruct. **24**, 409 (1998); A. W. Sleight, Physica C **514**, 152 (2015).

[14] J. F. Schooley, W. R. Hosler and M. L. Cohen, Phys. Rev. Lett. **12**, 474 (1964); R. M. Fernandes, J. T. Haraldsen, P. Wölfle, and A. V. Balatsky, Phys. Rev. B **87**, 014510 (2013); D. Valentinis, D. van der Marel, and C. Berthod, Phys. Rev. B **94**, 024511 (2016); S. Kanasugi and Y. Yanase, Phys. Rev. B **100**, 094504 (2019); C. Collignon, X. Lin, C. W. Rischau, B. Fauque, and K. Behnia, Annu. Rev. Condens. Matter Phys. **10**, 25 (2019).

[15] A. S. Alexandrov and N. F. Mott, "Polarons and Bipolarons", World Scientific, Singapore, (1995), and references therein.

[16] We do not discuss the high-temperature superconductivity in sulfur hydrides under high pressure, see A. P. Drozdov *et al.* , Nature 525, 73 (2015) because we are interested in supercon-

ductivity at ambient pressure.

[17] S. Barisić, J. Labbé, and J. Friedel, Phys. Rev. Lett. **25**, 919 (1970).

[18] S. Barisić, Phys. Rev. B **5**, 932 (1972); **5**, 941 (1972).

[19] W. P. Su, J. R. Schrieffer, and A. J. Heeger, Phys. Rev. Lett. **42**, 1698 (1979).

[20] A. J. Heeger, S. Kivelson, J. R. Schrieffer, and W. P. Su, Rev. Mod. Phys. 60, 781 (1988)

[21] T. Holstein, Ann. Phys. (NY) **8**, 325 (1959); **8**, 343 (1959).

[22] H. Fröhlich, Adv. Phys. **3**, 325 (1954); S. I. Pekar, E. I. Rashba, and V. I. Sheka, Zh. Eksp. Teor. Fiz. **76**, 251 (1979); [Sov. Phys. JETP **49**, 129 (1979)]; I. M. Dykman and S. I. Pekar, Dokl. Akad. Nauk SSSR **83**, 825 (1952).

[23] D. Marchand, G. De Filippis, V. Cataudella, M. Berciu, N. Nagaosa, N. V. Prokof'ev, A. S. Mishchenko, and P. C. E. Stamp, Phys. Rev. Lett. **105**, 266605 (2010).

[24] John Sous, Monodeep Chakraborty, Roman V. Krems and Mona Berciu, Phys. Rev. Lett. **121**, 247001 (2018).

[25] J. Sous, "Peierls bipolarons and localization in solid-state and molecular systems", Ph.D. Thesis, University of British Columbia 2018

[26] see, for instance, D. van der Marel, F. Barantani, and C. W. Rischau, Phys. Rev. Research **1**, 013003 (2019); Arash Khazraie, Kateryna Foyevtsova, Ilya Elfimov, and George A. Sawatzky, Phys. Rev. B **97**, 075103 (2018).